NIH Public Access
Author Manuscript
Nat Commun. Author manuscript; available in PMC 2014 March 04.

Published in final edited form as:
Nat Commun. 2013 ; 4: 2354. doi:10.1038/ncomms3354.

MG53-induced IRS-1 ubiquitination negatively regulates skeletal myogenesis and insulin signaling

Jae-Sung Yi[1], **Jun Sub Park**[1], **Young-Mi Ham**[1], **Nga Nguyen**[1], **Na-Rae Lee**[1], **Jin Hong**[1], **Bong-Woo Kim**[1], **Hyun Lee**[1], **Chang-Seok Lee**[1], **Byung-Cheon Jeong**[1], **Hyun Kyu Song**[1], **Hana Cho**[1], **Yoon Ki Kim**[1], **Jae-Seon Lee**[2], **Kyong-Soo Park**[3], **Hakseob Shin**[4], **Inho Choi**[4], **Seung Hee Lee**[5], **Woo Jin Park**[5], **Shi-Young Park**[6], **Cheol Soo Choi**[6,7], **Peihui Lin**[8], **Malith Karunasiri**[8], **Tao Tan**[8], **Pu Duann**[8], **Hua Zhu**[8], **Jianjie Ma**[8], and **Young-Gyu Ko**[1,¶]

[1]Department of Life Sciences, Korea University, Seoul, 136-701, Korea

[2]Division of Radiation Cancer Research, Korea Institute of Radiological and Medical Sciences, Seoul, 139-706, Korea

[3]Department of Internal Medicine, Seoul National University College of Medicine, Seoul, 110-799, Korea

[4]Division of Biological Science and Technology, Yonsei University, Wonju, Gangwon-Do, 220-710, Korea

[5]College of Life Sciences, Gwangju Institute of Science and Technology, Gwangju, 500-712, Korea

[6]Korea Mouse Metabolic Phenotyping Center, Lee Gil Ya Cancer and Diabetes Institute, Incheon, 406-840, Korea

[7]Department of Internal Medicine, Gil Medical Center, Gachon University, Incheon, 406-840, Korea

[8]Department of Surgery, Division of Surgical and Biomedical Sciences, Davis Heart and Lung Research Institute, The Ohio State University, Columbus, OH 43210, USA

Abstract

Mitsugumin 53 (MG53) negatively regulates skeletal myogenesis by targeting insulin receptor substrate 1 (IRS-1). Here, we show that MG53 is a ubiquitin E3 ligase that induces IRS-1 ubiquitination with the help of an E2-conjugating enzyme UBE2H. Molecular manipulations that disrupt the E3 ligase function of MG53 abolishes IRS-1 ubiquitination and enhances skeletal myogenesis. Skeletal muscles derived from the MG53$^{-/-}$ mice show an elevated IRS-1 level with enhanced insulin signaling, which protects the MG53$^{-/-}$ mice from developing insulin resistance when challenged with a high fat/high sucrose diet. Muscle samples derived from human diabetic patients and mice with insulin resistance show normal expression of MG53, indicating that altered MG53 expression does not serve as a causative factor for the development of metabolic disorders.

¶To whom correspondence should be addressed: Young-Gyu Ko, Ph. D., Department of Life Sciences, Korea University, 145, Anam-ro, Seongbuk-gu, Seoul, 136-701, Korea, ygko@korea.ac.kr; TEL: 82-2-3290-3453; FAX: 82-2-927-9028.

Author contributions

J.-S. Y., J.-s. P., Y.-M. H., N. N., H. J., N.-R. L., B.-W. K., H. L., J.-J. P., C.-S. L., B.-C. J., H. C., H. S., S.-H. L., P. L., M. K., T. T., T. D. and S.-Y. P. performed experiments; K.-S. P. collected human skeletal muscles; H.-K. S., Y.-K. K., J.-S. L., I. C., W.-J. P., C.-S. C., H. Z., J. M., and Y.-G. K. designed experiments and analyzed data; and J.-S. Y., H. Z., J. M., and Y.-G. K. wrote the manuscript.

Conflict of interest

The authors declare no competing financial interests.

NIH-PA Author Manuscript
NIH-PA Author Manuscript
NIH-PA Author Manuscript

NIH-PA Author Manuscript

NIH-PA Author Manuscript

NIH-PA Author Manuscript

Thus, therapeutic interventions that target the interaction between MG53 and IRS-1 may be a novel approach for the treatment of metabolic diseases that are associated with insulin resistance.

Introduction

Skeletal muscle comprises about 40% of the human body mass and is a major organ that is necessary for locomotion and glucose homeostasis. Adult skeletal muscle mass is plastically regulated by recruiting satellite cells to preexisting muscle fibers under hypertrophic conditions such as resistance and endurance exercise [1,2]. Skeletal muscle differentiation, hypertrophy, and atrophy are tightly regulated by a variety of hormones, growth factors and cytokines. In particular, insulin-like growth factor-I (IGF-1), plays a key role in the regulation of skeletal muscle size. IGF-1 knockout mice exhibit muscle hypoplasia and die shortly after birth due to impaired respiration [3,4,5]. *In vivo* injection of IGF-1 in skeletal muscle or skeletal muscle-specific overexpression of IGF-1 results in larger muscle fibers with enhanced muscle performance [6,7]. Interestingly, IGF-1 production and secretion are increased by muscle hypertrophy-inducing hormones (e.g., catecholamine and leptin) but decreased by muscle atrophy-inducing hormones (e.g., TGFβ, myostatin and glucocorticoid) [8,9,10,11].

IGF-1 leads to the consecutive activation of IGF receptor (IGFR), insulin receptor substrate (IRS), phosphatidylinositol 3-kinase (PI3K), Akt, mammalian target of rapamycin (mTOR) and S6 kinase (S6K), which together orchestrate skeletal myogenesis and hypertrophy [12,13,14,15]. Studies with skeletal muscle-specific knockout and transgenic mice for Akt, mTOR or S6K show that the Akt-mTOR-S6K signaling axis is essential for skeletal muscle hypertrophy and regeneration [16,17]. IGF-1-mediated Akt activation blocks the transcription factor forkhead box family proteins (FOXO1 and FOXO3A) by phosphorylating and sequestering them in the cytoplasm [18,19]. Because the target genes for FOXO proteins are E3 ubiquitin ligases such as atrogin-1 and muscle-upregulated RING finger-1 (MURF-1) in the skeletal muscle, Akt-mediated FOXO inactivation inhibits the ubiquitin-proteasome system (UPS), which is essential for the degradation of myofibrillar, metabolic, and transcriptional proteins [20,21,22]. Indeed, knockout mice for either atrogin-1 or MURF-1 are resistant to atrophy [21].

The UPS for protein degradation is necessary for the regulation of skeletal muscle differentiation, hypertrophy and atrophy [23,24]. Ubiquitin (Ub) and E1 ubiquitin activating, E2-conjugating and E3 Ub-ligase enzymes are required for polyubiquitinating a specific target protein. The E3 ligases have two major types, HECT (homologous to E6AP carboxyl terminus) ligases and RING (really interesting new gene) finger ligases [25]. The tripartite motif-containing (TRIM) superfamily is composed of 77 human proteins with a RING finger domain, one or two B-boxes, and one or two coiled-coil domains [26]. TRIM proteins have a plethora of biological functions related to cellular signal transduction and differentiation, transcriptional and cell cycle regulation and innate anti-viral activity [26]. Due to their RING finger domain with E3 ligase activity, the TRIM superfamily proteins are essential for the ubiquitination of their specific target protein prior to executing their cellular function.

MG53, also known as TRIM72, was identified in C2C12 myotubes by comparative two-dimensional electrophoresis of detergent-resistant lipid rafts, which work as a signal transduction center [27,28]. MG53 expression gradually increases during the myogenesis of C2C12 and satellite cells, because its promoter contains E-boxes and MEF-binding sites for the myogenic transcription factors, MyoD and MEF, respectively [28,29]. MG53 is recruited to lipid rafts, where it associates with and inactivates IRS-1, leading to the negative feedback regulation of skeletal myogenesis. In addition, MG53 acts as a major regulator for

NIH-PA Author Manuscript

NIH-PA Author Manuscript

NIH-PA Author Manuscript

membrane repair by interacting with dysferlin-1, caveolin-3 and cavin-1 [30,31,32]. Indeed, the muscle fibers of MG53$^{-/-}$ mice show membrane repair defects[31]. Although MG53 might be a putative E3 ligase due to its RING domain, there has been no report of its function as an E3 ligase in either skeletal myogenesis or membrane repair. Here, we demonstrate that MG53 induces IRS-1 ubiquitination with the help of the E2 enzyme UBE2H during skeletal myogenesis by examining MG53-disrupted skeletal muscle cells and tissues. We find that knocking out the MG53 gene in mice ameliorates high fat/high sucrose diet-induced insulin resistance by increasing the IRS-1 expression level and insulin signaling in skeletal muscle. We also find that MG53 protein level is not upregulated in the muscle samples derived from mice and human patients with metabolic disorders, suggesting that MG53 upregulation is not a causative factor for the development of insulin resistance. Based on these observations, we propose that therapeutic interventions that target direct interaction between MG53 and IRS-1 without disruption of membrane repair function for MG53 may be a novel approach for the treatment of metabolic disorders that are associated with insulin resistance.

Results

MG53 RING domain regulates skeletal myogenesis

MG53 has been hypothesized to be an E3 ligase because it has an evolutionarily conserved RING domain (Supplementary Fig. S1a) [26,28,31,33]. To elucidate the role of the MG53 RING domain in skeletal myogenesis, we prepared two human MG53 mutants: MG53 C14A, in which the critical cysteine at position 14 was mutated to alanine and ΔR, a MG53 mutant devoid of the RING domain (Supplementary Fig. S1b). C2C12 myoblasts were infected with adenovirus harboring MG53 or the C14A or ΔR mutant and then were differentiated to myotubes for 4 days. Myogenesis was determined by immunofluorescence for myosin heavy chain (MyHC), the myogenic index and immunoblotting for myogenic marker proteins including MyHC, caveolin-3 (Cav-3) and myogenin (Mgn). As shown in Fig. 1a–c, myogenesis was blocked by MG53 overexpression but was enhanced with the C14A or ΔR mutant. Transient non-viral overexpression of Flag-MG53, C14A or ΔR in C2C12 cells also provided similar results during myogenesis (Supplementary Fig. S1c).

Next, we examined IGF-1 signaling after adenoviral infection of MG53, C14A or ΔR in C2C12 myoblasts or myotubes. As shown in Fig. 1d and Supplementary Fig. S2 a–c, MG53 overexpression reduced IGF-1-elicited IRS-1 tyrosine phosphorylation and Akt phosphorylation without affecting IGF-1-elicited IGFR tyrosine phosphorylation and ERK1/2 phosphorylation. It should be noted that IGF-1 activates ERK1/2 through an IGFR-Ras-Raf pathway but not through an IGFR-IRS-1 pathway [34,35]. These data suggest the possibility that IRS-1 could be a molecular target of MG53. Interestingly, the IGF-1-elicited IRS-1 and Akt activation was increased in C2C12 myotubes following transient infection with C14A or ΔR. These results suggest that the RING domain of MG53 is necessary for the inhibition of IGF-1-elicited IRS-1 phosphorylation.

MG53 is a ubiquitin E3 ligase that targets IRS-1

Co-immunoprecipitation studies revealed that MG53 was physically interacted with IRS-1 and mutations in the RING domain of MG53 did not affect the binding of MG53 to IRS-1 in HEK 293 cells overexpressing IRS-1 and either MG53, C14A or ΔR (Supplementary Fig. S3a). In contrast, the IRS-1 expression level was decreased about 60% by MG53 but not by C14A or ΔR in both C2C12 myoblasts and myotubes (Fig. 1d; Supplementary Fig. S2d). Although the IRS-1 mRNA level was slightly increased, its protein level gradually decreased during C2C12 myogenesis when MG53 expression was induced (Fig. 2a–c), whereas the protein levels of insulin receptor β (IRβ)and IGFR did not appear to change during C2C12 myogenesis.

NIH-PA Author Manuscript

NIH-PA Author Manuscript

NIH-PA Author Manuscript

To examine the mechanisms underlying the MG53-mediated down-regulation of IRS-1, we used the transient expression of IRS-1 and MG53 in HEK 293 cells. The IRS-1 protein level was decreased by MG53 in a concentration-dependent manner (Supplementary Fig. S3b) and was restored by the addition of MG132, a proteasome inhibitor (Fig. 2d; Supplementary Fig. S3c). However, the proteasomal degradation of IRS-1 was not induced by the C14A and ΔR mutants, even in the absence of MG132 (Fig. 2e,f), suggesting that the RING domain of MG53 is essential for the proteasomal degradation of IRS-1.

We also determined the stability of the IRS-1 protein in C2C12 myotubes following siRNA-mediated knockdown of MG53 by pulse-chase labeling. As shown in Fig. 2g,h, the specific siRNA could downregulate more than 90% of MG53 expression, leading to threefold increase of half-life time of the IRS-1 protein. To study MG53-mediated IRS-1 ubiquitination, we co-expressed IRS-1, ubiquitin with either MG53, C14A or ΔR and found that neither C14A nor ΔR could induce ubiquitination even in the presence of MG132 (Fig. 2i). Because the lysis buffer for IRS-1 immunoprecipitation contained a strong detergent, the ubiquitination signal was from IRS-1 but not from MG53. Next, we tested whether the RING domain of MG53 is indispensable for IRS-1 ubiquitination in C2C12 myoblasts after adenoviral infection of MG53, C14A or ΔR. As shown in Fig. 2j, IRS-1 ubiquitination was again induced by MG53 but not by C14A or ΔR in the presence of MG132. Moreover, IRS-1 ubiquitination and degradation were abolished by MG53 knockdown in C2C12 myotubes (Fig. 2k).

Because IRS-2 also mediates IGF-1 signaling in skeletal muscle, we investigated MG53-dependent IRS-2 ubiquitination. As shown in Supplementary Fig. S3 d,e, the IRS-2 expression level and ubiquitination were not changed by MG53 overexpression in myoblasts or MG53 knockdown in myotubes. These data indicate that MG53 is a true E3 ligase enzyme for the ubiquitination of IRS-1 and not IRS-2.

C14A and ΔR mutants of MG53 do not degrade IRS-1

Further studies showed the C14A and ΔR mutants function as a dominant-negative form of MG53 in IRS-1 degradation. Myc-MG53 was shown to be associated with Flag-MG53, C14A and ΔR by reciprocal exogenous immunoprecipitation of HEK 293 cells (Supplementary Fig. S4a,b). Moreover, MG53, C14A and ΔR appeared to be oligomerized in the presence of glutaraldehyde, a protein cross-linker (Supplementary Fig. S4c), suggesting that the RING domain is not necessary for MG53 oligomerization. We found that MG53-induced IRS-1 degradation was completely abolished by C14A or ΔR mutant in HEK 293 cells (Supplementary Fig. S4d). These data demonstrate that these RING domain-disrupted MG53 mutants (C14A and ΔR) function as a dominant negative form of MG53 via their oligomer formation with MG53 and then enhance skeletal myogenesis by abrogating MG53-induced IRS-1 ubiquitination (Fig. 1, 2).

To further confirm the effect of MG53 on myogenesis and IRS-1 ubiquitination, mouse embryonic fibroblasts (MEFs) were obtained from $MG53^{+/+}$ and $MG53^{-/-}$ mouse embryos and were differentiated to myotubes after adenoviral MyoD overexpression. The MG53 protein level increased, along with other myogenic marker proteins such as MyHC, Cav-3 and Mgn, but the IRS-1 protein level decreased during MyoD-driven myogenesis in $MG53^{+/+}$ MEFs (Fig. 3a). As evidenced by MyHC immunofluorescence, myogenic index and immunoblotting, MG53 knockout enhanced myogenesis by increasing the level of IRS-1 expression (Fig. 3b–d). We also found that MG53 knockout abolished IRS-1 ubiquitination in the MyoD-driven myotubes of MEFs (Fig. 3e), supporting the concept that MG53 is an E3 ligase for IRS-1.

NIH-PA Author Manuscript

NIH-PA Author Manuscript

NIH-PA Author Manuscript

UBE2H is involved in MG53-mediated IRS-1 ubiquitination

Because a specific ubiquitin-conjugating E2 enzyme transfers ubiquitin to a specific target protein through E3 ligase [36], MG53-mediated IRS-1 ubiquitination should have an E2 enzyme partner. To identify the ubiquitin-conjugating E2 enzyme for MG53, we examined the molecular association of MG53 with various E2 enzymes. As shown in *in vitro* binding assay (Supplementary Fig. S5a; Fig. 4a), MG53 strongly interacted with UBE2H. The UBE2H mRNA and protein levels gradually increased along with MG53 expression during C2C12 myogenesis (Supplementary Fig. S5b–d). The physical association of UBE2H with MG53 was further confirmed by exogenous co-immunoprecipitation studies in HEK 293 cells that overexpress UBE2H and MG53 and by reciprocal endogenous immunoprecipitation in C2C12 myotubes (Fig. 4b,c). Thus, UBE2H appears to be a good candidate for the E2-conjugating enzyme for MG53.

The role for UBE2H in myogenesis was tested in C2C12 cells following siRNA-mediated knockdown. As shown in Fig. 4d–f, C2C12 myogenesis was enhanced by UBE2H knockdown, where the IRS-1 expression level was increased about 3-fold and IRS-1 ubiquitination was abolished in C2C12 myotubes (Fig. 4f,g). To test whether the MG53 inhibition of myogenesis is reversed by UBE2H knockdown, HA-MG53 was transiently transfected along with si-control or si-UBE2H (200 nM) in C2C12 myoblasts, which were further differentiated to myotubes. Clearly, assessment of myogenesis by immunofluorescence for HA and MyHC and myogenic index revealed that the MG53-induced inhibition of myogenesis was abolished by UBE2H knockdown (Fig. 4h,i). In addition, the MG53-induced IRS-1 ubiquitination was further increased by UBE2H overexpression in HEK 293 cells (Supplementary Fig. S5e). These data suggest that UBE2H is a genuine E2-conjugating enzyme for MG53.

MG53 expression affects insulin signaling in cultured C2C12 myotubes

To test whether the MG53-mediated control of IRS-1 expression may contribute to insulin signaling in skeletal muscle, we monitored insulin-elicited IRS-1, Akt and ERK1/2 phosphorylation in MG53-overexpressing C2C12 myoblasts. As shown in Fig. 5a,b and Supplementary Fig. S6, insulin-elicited IRS-1, Akt and ERK1/2 activation was dramatically decreased by MG53 overexpression. In contrast to IGF-1 signaling, IRS-1 is required for insulin-elicited ERK1/2 activation [14,37]. These data indicate that MG53 negatively regulates insulin signaling. Because the IRS-1 protein level was decreased during myogenesis (Fig. 2c, 3a), insulin signaling might also be down-regulated in myotubes, compared with myoblasts. Indeed, myotubes had less insulin-elicited phosphorylation of IRS-1, Akt and ERK1/2 than myoblasts did, whereas both cells had no difference in insulin-elicited IRβ phosphorylation (Fig. 5c). However, myotubes had greater insulin-induced glucose uptake than myoblasts did (Supplementary Fig. S7) because of the higher expression level of GLUT4 in the myotubes [38,39,40].

Systemic MG53 disruption improves muscle insulin signaling

Insulin signaling was also analyzed in the soleus and gastrocnemius-plantaris muscles of 8-week-old $MG53^{-/-}$ mice after the intravenous injection of insulin. In both muscles, the increase of insulin-elicited IRS-1, Akt and ERK1/2 activation was observed along with an elevation in the IRS-1 expression level in $MG53^{-/-}$ mice, compared with $MG53^{+/+}$ mice (Fig. 5d,e). However, there was no difference in IRβ protein expression level and insulin-elicited IRβ activation between skeletal muscles obtained from $MG53^{+/+}$ and $MG53^{-/-}$, indicating that IRβ is not a substrate of E3 ligase MG53.

The 8-week-old $MG53^{-/-}$ mice did not show pathological cardiac hypertrophy and alterations in total body weight, locomotion activity and muscle fiber type composition

NIH-PA Author Manuscript

NIH-PA Author Manuscript

NIH-PA Author Manuscript

(Supplementary Fig. S8,S9). Because MG53 has been reported to be highly expressed in soleus muscle compared to other skeletal muscles[29], we speculated that the change of muscle fiber size by MG53 knockout might appear in the soleus. Indeed, only soleus muscle of MG53$^{-/-}$ mice was approximately 27% heavier than that of MG53$^{+/+}$ mice, while there were no differences in GP and TA muscle weight (Supplementary Fig. S10a). The cross-sectional area was increased in the soleus muscle but was similar in the GP and TA of MG53$^{-/-}$ mice (Supplementary Fig. S10b–e), compared with those of MG53$^{+/+}$. In addition, higher muscle fatigue resistance was shown in the soleus but not in extensor digitorum longus (EDL) of MG53$^{-/-}$ mice, compared with those of MG53 $^{+/+}$(Supplementary Fig. S11).

We also analyzed muscular hypertrophy and insulin signaling in 38-week-old MG53$^{-/-}$ mice. The older MG53$^{-/-}$ mice did not show muscular hypertrophy any more (Supplementary Fig. S12a,b). However, IRS-1 expression level and insulin-elicited IRS-1, Akt and ERK1/2 phosphorylation were still increased in the skeletal muscles of MG53$^{-/-}$ mice, compared with those of MG53$^{+/+}$mice (Supplementary Fig. S12c,d).

The increased insulin signaling in skeletal muscle might lead to insulin-sensitive phenotypes in MG53$^{-/-}$ mice. Although there was no difference in whole body weight, fat mass, food intake, energy expenditure and locomotor activity between high-fat diet-fed MG53$^{+/+}$ and MG53$^{-/-}$ mice (Supplementary Fig. S13), the serum levels of triacylglycerol, free fatty acid, total cholesterol, insulin and leptin were dramatically lower in high fat/high sucrose (HF/HS)-fed MG53$^{-/-}$ mice, compared with HF/HS-fed MG53$^{+/+}$ mice (Fig. 6a–e). Glucose disposal rates during the glucose and insulin tolerance test were improved from MG53$^{-/-}$ mice fed with both of regular and HF/HS diet compared with regular and HF/HS diet-fed MG53$^{+/+}$mice, respectively (Fig. 6f,g).

Since inflammation in adipose tissues induces insulin resistance [41,42,43,44], we next monitored the effect of MG53 disruption on the inflammation status by measuring mRNA levels of inflammatory cytokines (IL1β, PAI and TNF-α) and by immunofluorescence of macrophage infiltration markers (F4/80 and MCP-1) in the epididymal adipose tissue obtained from HF/HS-fed MG53$^{+/+}$ and MG53$^{-/-}$ mice. As shown in Supplementary Fig. S14a, there was no difference in the mRNA levels between HF/HS-fed MG53$^{+/+}$ and MG53$^{-/-}$ mice. Moreover, HF/HS-fed MG53$^{+/+}$ and MG53$^{-/-}$ mice had similar macrophage infiltration into adipose tissue (Supplementary Fig. S14b). These data indicate that MG53 disruption ameliorates HF/HS-induced insulin resistance without preventing fat mass increase and macrophage infiltration in adipose tissue from HF/HS-fed mice.

MG53 in animal models and humans with metabolic disorders

A recent study by Song et al. [53] showed that MG53 protein level is upregulated in the skeletal muscles obtained from multiple animal models for metabolic disorders. In particular, they reported that skeletal muscle derived from the *db/db* mice at 25 weeks of age exhibited greater than 3-fold upregulation of MG3 protein when compared with the lean mice and feeding of mice with high-fat diet (HFD) led to several fold upregulation of MG53, as early as one week following HFD treatment. These were the main experimental evidence supporting their conclusion that MG53 upregulation serves as a causative factor for metabolic disorders.

We performed immunoblotting with skeletal muscle derived from *db/db* and their littermate lean control mice and found no significant difference in MG53 expression in both slow-twitch soleus and fast-twitch extensor digitorum longus (EDL) muscle at 22–29 weeks of age (Fig. 7a). Similar protein levels for MG53 were also observed between the *ob/ob*, *db/db* and age-matched lean control mice at 8-week age when the *db/db* mice already develop

NIH-PA Author Manuscript

NIH-PA Author Manuscript

NIH-PA Author Manuscript

metabolic disorder (Fig. 7b). We next assayed the expression of MG53 using skeletal muscle biopsies obtained from the type 2 diabetic human patients. As shown in Fig. 7c, while the level of MG53 protein may vary from different patients, immunoblotting revealed no significant changes in MG53 expression among the different age and gender groups between the healthy people and diabetic patients. Thus, our human muscle data do not reveal a correlation between changes in MG53 expression and diabetic disorder.

We also found negligible changes in expression of MG53 in skeletal muscle following three different paradigms of high fat diet (HFD) treatment (Fig. 7d). First, when the wild type mice were treated with HFD or regular Chow diet (RD) for 1 week starting right after their weaning age (25 days after birth), such acute HFD-treatment did not alter the expression for MG53 in skeletal muscle (Fig. 7d, *top*). Second, to test whether development of the mice can impact the effect of HFD on MG53 expression in skeletal muscle, we treated mice with HFD for 1-week starting at the adolescent age (8-week old). Again, there were no significant changes in MG53 expression between RD- and HFD-treated mice (Fig. 7d, *middle*). Third, when the adolescent mice were subjected to 4-weeks of HFD treatment, there were not significant changes in MG53 expression in skeletal muscle (Fig. 7d, *bottom*).

Overall, our data show that MG53 is not upregulated in the skeletal muscles from animals and human patients with metabolic disorders, arguing against the claim made by Song et al. [53].

Discussion

Here, we provide multiple lines of evidence to show that MG53 is a negative feedback regulator of myogenesis and insulin signaling in skeletal muscle. First, we showed that MG53 overexpression blocked myogenesis, while RNAi-mediated silencing of MG53 accelerated myogenesis by modulating IGF-1-elicited IRS-1, PI3K and Akt activation [28]. Second, we found that overexpression of RING domain-disrupted MG53 mutants (C14A and ΔR) led to disruption of MG53-mediated IRS-1 ubiquitination and consequently the robust muscle differentiation (Fig. 1,2). Such dominant negative effect of the MG53 mutants provide an attractive avenue for pharmacological or molecular manipulations that can be used to target the intermolecular interactions among MG53 and its target molecules for treatment of metabolic diseases linked to muscle dysfunctions. Third, we provide conclusive evidence that links myogenesis enhancement with increased level of IRS-1 in MyoD-driven $MG53^{-/-}$ myotubes and the $MG53^{-/-}$ mice (Fig. 3,5). Together, our data indicate that MG53 is a real E3 ligase enzyme that is required for IRS-1 ubiquitination to negatively regulate skeletal muscle myogenesis and insulin signaling.

Based on the above findings, we propose the following model for MG53 as a negative feedback regulator of IGF-1 signaling during skeletal myogenesis (Fig. 8). In myoblasts that do not express MG53 (Fig. 8, **left panel**), IGF-1 initiates myogenesis via the IGFR-IRS-PI3K-Akt-MyoD signaling pathway. IGF-1-elicited Akt activation leads to phosphorylation of p300, causing an association of MyoD with p300 and PCAF acetyltransferases [45]. The activated muscle transcriptosome binds to the MG53 promoter with E-box and MEF-binding sites and then initiates MG53 transcription [29]. MG53 protein begins to accumulate in the sarcolemma and associates with and polyubiquitinates IRS-1 with the help of UBE2H. The polyubiquitinated IRS-1 is degraded by the ubiquitin-proteasome system. Thus, in fully differentiated myotubes with forced expression of MG53 (Fig. 8, **right panel**), the IGF-1-elicited Akt activation is weakened due to the low IRS-1 level, which is caused by the UBE2H-MG53-proteasome system. However, IGF-1-elicited Erk1/2 activation is not influenced by MG53 in either myoblasts or myotubes because the Ras-Raf-Erk1/2 pathway is diverted from IGFR [34,35], whose expression level and activity are not changed by MG53.

NIH-PA Author Manuscript

NIH-PA Author Manuscript

NIH-PA Author Manuscript

Because IRS-1 is a convergent signal molecule for IGF-1 and insulin signaling, IRS-1 deficiency abolishes skeletal myogenesis and insulin signaling. Lee et al. showed that MG53 knockdown-induced myogenesis enhancement is completely abrogated by IRS-1 knockdown, indicating that IRS-1 is a downstream signaling molecule of MG53 that is required for the negative regulation of myogenesis [27,28]. In addition, IRS-1 knockout mice show insulin resistance and no IGF-1-induced muscle growth [46,47,48]. These findings indicate that IRS-1 is essential for insulin signaling and IGF-1-mediated muscle growth. To investigate MG53-dependent myogenesis inhibition and insulin signaling, we monitored C2C12 differentiation and insulin signaling after MG53 overexpression. IGF-1 and insulin signaling and myogenesis were decreased after MG53 overexpression (Fig. 1,5). Thus, our data suggest that both MG53-dependent myogenesis inhibition and insulin insensitivity are tightly related with IRS-1.

IRS-1 is polyubiquitinated and degraded by SOCS1/3, Cbl-b, Cul7 and SCF-Fbxo40. SOCS1/3 is activated by inflammation and might induce insulin resistance in the liver by polyubiquitinating IRS-1 and IRS-2 [49]. Cbl-b targets IRS-1 during muscular atrophy such as unloading [50]. Cul7-induced IRS-1 polyubiquitination might contribute to the regulation of oncogene-induced senescence [51]. Skeletal muscle-specific Fbxo40 interacts with and ubiquitinates IRS-1 during skeletal myogenesis [52]. However, there is no direct evidence to date that connects these E3 ligases with insulin resistance.

Recently, Song *et al*. claimed that MG53 protein expression level is highly increased in the skeletal muscle obtained from high fat diet-fed and *db/db* mice, spontaneously hypertensive rats, nonhuman primates with metabolic syndrome and human obese patients, concluding that upregulation of MG53 serves as a universal causative factor for development of metabolic diseases in skeletal muscle[53]. However, our data showed that MG53 upregulation in skeletal muscle was not observed from *ob/ob*, *db/db* and HFD-fed mice and type 2 diabetes patients(Fig. 7), challenging the conclusion that MG53 upregulation serves as a preceding factor for the development of metabolic disorders. Song et al. also claimed that IRβ is ubiquitinated by MG53 because that IRβ ubiquitination and insulin-elicited IRβ phosphorylation are increased in MG53 transgenic mice and abolished in MG53 knockout mice[53]. However, our data showed that IRβ might not be a substrate of E3 ligase MG53 because IRβ protein level or insulin-elicited IRβ phosphorylation were not changed during C2C12 myogenesis when MG53 protein level was gradually increased (Fig. 2c), by MG53 overexpression in C2C12 myoblasts (Fig. 5a–c) or by systemic MG53 disruption (Fig. 5d,e). These data challenge the MG53-induced IRβ degradation observed by Song et al. [53]

We showed that MG53 disruption increased insulin-elicited IRS-1 activation with an elevated IRS-1 protein level in mouse skeletal muscle, inducing skeletal muscle hypertrophy at least in the soleus, improving glucose tolerance even in regular diet-fed mice and ameliorating HF/HS diet-induced insulin resistance (Fig. 5 and 6). Thus, we can conclude that the inhibition of MG53-mediated IRS-1 ubiquitination could be used as a therapeutic strategy for the treatment of muscular atrophy and insulin resistance. Since MG53 has dual functions as an E3 ligase that targets ubiquitination-mediated degradation of IRS-1 and an indispensable component of the cell membrane repair machinery [30, 31], compounds that prevent the molecular association of MG53 with IRS-1 or UBE2H without disruption of the membrane repair function for MG53 might be developed as drug candidates for the treatment of insulin resistance. Alternatively, molecular interventions that selectively abolish the E3-ligase function for MG53 without impacting the tissue repair function for MG53 could be an attractive avenue for development of MG53 as a therapeutic reagent for regenerative medicine [57].

NIH-PA Author Manuscript

NIH-PA Author Manuscript

NIH-PA Author Manuscript

Methods

Generation of MG53$^{-/-}$ mice

MG53$^{-/-}$ mice were generated as described previously [28]. Briefly, exons 1, 2 and 3 of the TRIM72 gene were replaced with a PGK-neo sequence within the targeting vector by homologous recombination. For screening of recombination-positive embryonic stem cells, genomic DNA was digested with *Bam*HI, and analyzed by Southern blotting. To backcross the mice, MG53$^{+/-}$ mice were bred with C57BL/6 mice for 7 generations. Mice were housed in plastic cages under a 12:12 h light-dark photoperiod with free access to water and food. To induce insulin resistance, the 4-week-old male mice were fed with a high-fat and high-sucrose (HF/HS) diet (35.8 % (w/w) fat, 35.5 % (w/w) carbohydrate and 23.0 (w/w) protein; D12331, Research Diet, New Brunswick, NJ) for 10 weeks. Animals were handled according to the Principles of Laboratory Animal Care (NIH Publication No. 85-23, revised 1985), and the protocols were approved by the Institutional Animal Care and Use Committee of Korea University.

Cell culture

C2C12 cells were purchased from ATCC and grown in growth medium (Dulbecco's modified Eagle's medium supplemented with 2% penicillin/streptomycin and 10% feral bovine serum) in a 5% CO_2 incubator at 37°C. Confluent C2C12 myoblasts were differentiated into myotubes by incubation with differentiation medium (DMEM supplemented with the same antibiotics as above and 2% horse serum). Every 48 h, the myotubes were fed with fresh differentiation medium. Mouse embryonic fibroblasts (MEFs) were obtained from MG53$^{+/+}$ and MG53$^{-/-}$ embryos at embryonic day 12.5 according to Shim et al. [54]. To differentiate the cells into myotubes, MEFs were transfected with adenoviral MyoD (5x10^9 VP/ml) for 12 h and incubated with differentiation medium.

Adenoviral preparation and infection

Adenoviruses harboring MG53, C14A and ΔR were produced according to a previously described method[28]. Adenovirus containing MyoD was obtained from Cell Biolabs (San Diego, CA). To amplify the virus, viral stocks were reinfected into AD293 cells and purified by double cesium chloride-gradient ultracentrifugation. Infectious viral particles (VPs) in the cesium chloride gradient (density = approximately 1.345) were collected, dialyzed against 10 mM Tris (pH 8.0), 2 mM $MgCl_2$ and 5% sucrose solution and stored at −80°C. C2C12 myoblasts or MEFs were infected by adenovirus at a dosage of 5x10^9 VP/ml.

Plasmids for transient transfection and luciferase assay

Human IRS-1, ubiquitin and MG53, C14A and ΔR cDNA constructs were generated by PCR and cloned into the pCMV-Tag2b and pCMV-3Tag4a vectors. DNA transfection was performed using Polyfect (Qiagen, Valencia, CA) or electroporation (Invitrogen, Grand Island, NY) according to the manufacturer's protocol.

Antibody-based assays

Immunoblotting and immunofluorescence were performed according to Yi et al. [55]. For immunoblotting, proteins were separated on polyacrylamide gel and transferred onto a PVDF membrane. The membranes were then blocked for 1 hr at room temperature, and allowed to react with a sequence of primary and secondary antibodies. The antigen signals were visualized using ECL reagents. For immunofluorescence, cells were fixed with 3.7% formaldehyde for 10min, permeabilized with 0.1% TX-100 in PBS, washed 3 times with PBS and then blocked with 5% BSA in PBS for 1hr. After blocking cells were incubated with primary antibodies and primary antibodies were detected using fluorescence-

NIH-PA Author Manuscript

NIH-PA Author Manuscript

NIH-PA Author Manuscript

conjugated secondary antibodies. Cells were observed with a fluorescence microscope (Axioplan-2; Carl Zeiss, Oberkochen, Germany). For immunoprecipitation, the cells were lysed in a buffer containing 20 mM Tris-HCl (pH 7.4), 137 mM NaCl, 1 mM $MgCl_2$, 1 mM $CaCl_2$, 20 mM NaF, 10 mM $Na_4P_2O_7$, 1 mM Na_3VO_4, 1% NP-40, 1 mM PMSF, and a protease inhibitor cocktail (Roche, Mannheim, Germany). The whole cell lysates (500 μg protein) were incubated with specific antibodies for 90 min and then with 50 μl of a Protein A-Agarose bead (Roche, Mannheim, Germany) slurry for 90 min. The immunoprecipitates were analyzed by immunoblotting. For immunofluorescence, C2C12 cells were washed briefly with PBS. Supplementary Table S1 and S2 show the information of antibodies which were used for immunoblotting, immunoprecipitation and immunofluorescence.

Measurement of the myogenic index

Differentiated C2C12 cells or MEFs were stained with anti-MyHC antibody and DAPI and cell images were obtained under a fluorescence microscope (Axioplan-2; Carl Zeiss, Oberkochen, Germany). The myogenic index was determined as the ratio of the nuclei within MyHC-positive myotubes to the total nuclear number in the stained field.

RNA interference

siRNA oligomers targeting MG53 (si-MG53) or UBE2H (si-UBE2H) and a scrambled oligomer (si-control) was obtained from Ambion. The target sequence of MG53 was 5′-AAGCACGCCUCAAGACACAGC-3′, and the target sequence of UBE2H was 5′-CUAUGAUCUUACCAAUAUAtt-3′. C2C12 myoblasts were transfected with 100 nM of si-control, si-MG53 or si-UBE2H by electroporation (Invitrogen, Grand Island, NY) according to the manufacturer's protocol.

Chemical cross-linking

HEK 293 cells were harvested with 60 mM octyl-β-D-glucopyranoside in PBS. Whole cell lysates were mixed with the indicated concentrations of glutaraldehyde and incubated at 37°C for 20 min. The cross-linking reaction was stopped by adding 1.5 M Tris-HCl (pH 7.4) and then the proteins were separated on SDS-PAGE.

In vitro binding assay

Human MG53 (residues 7-470) was cloned into the pMAL-c2x vector (NEB). *E. coli* C41(DE3) was used as an expression host strain for MBP-MG53. The expressed protein was purified using affinity column (amylose resin) followed by anion exchange chromatography (HiTrap Q Fast Flow column). Pull-down assays were carried out in 1 ml assay buffer (1X PBS and 1 mM DTT) containing 20 μl amylose resin, 50 μg MBP-MG53 and 100 μg His-tagged E2 enzymes for 1 h at 4°C. His-tagged E2 enzymes were purchased from Boston Biochem (Cambridge, MA) and LifeSensors (Malvern, PA). The interaction between MG53 and E2 enzymes was examined using immunoblotting with anti-His and anti-MBP antibodies.

Pulse chase analysis

C2C12 myoblasts were transfected with si-control or si-MG53 (40 nM) and differentiated for 4 days. The myotubes were incubated with methionin-free DMEM media (Sigma-Aldrich, St. Louis, MO) for 1 hr, pulsed with 10 μCi/ml of EasyTag™ EXPRESS^{35}S Protein Labeling Mix (Perkin-Elmer, Santa Clara, CA) for 2 hr and then chased with DMEM-containing 2% horse serum for the indicated times. Total cell lysates were immunoprecipitated with an anti-IRS-1 antibody and were separated by SDS-PAGE. ^{35}S-labeled IRS-1 was visualized by autoradiography.

NIH-PA Author Manuscript

NIH-PA Author Manuscript

NIH-PA Author Manuscript

RT-PCR

DNase1-treated RNA (1 μg) was converted to cDNA by reverse transcription using random hexamer primers and M-MLV reverse transcriptase (Invitrogen, Grand Island, NY). The PCR was initially performed over a range of cycles (24–38 cycles), and 2 μl of 1:4-diluted cDNA (12.5 ng/50 μl PCR reaction volume) undergoing 28–36 cycles was observed to be within the logarithmic phase of amplification and yielded reproducible results with the primers that are listed in Supplementary Table S3.

Quantitative real-time PCR

Quantitative real-time PCR analyses were performed using single-stranded cDNA and gene-specific oligonucleotides in the presence of the LightCycler 480 SYBR Green I Master Mix (Roche Diagnostics GmbH, Manheim, Germany). The LightCycler PCR conditions were as follows: an initial denaturation for 10 min at 95°C followed by 35–45 cycles of 95°C denaturation for 10 s, 57°C annealing for 10 s and 72°C elongation for 30 s. The melting curve of each PCR product was assessed for quality control.

IRS-1 ubiquitination

HEK 293T cells were co-transfected with Flag-IRS-1, His-Ubiquitin, and HA-MG53, C14A or HA-ΔR. After 32 h of transfection, the cells were treated with MG132 (2.5 μM) for 16 h and then harvested. The lysates were immunoprecipitated with an anti-Flag antibody, and the immunoprecipitates were immunoblotted with an anti-His antibody. Adenoviral MG53- or si-RNA-treated C2C12 cells were treated with MG132 (3 μM) for 16 hr and lysed with buffer containing 20 mM Tris (pH 7.5), 150 mM NaCl, 1 mM $MgCl_2$, 1 mM $CaCl_2$ and a protease inhibitor cocktail. Whole cell lysates were sonicated and subjected to immunoprecipitation with an anti-IRS-1 antibody. Endogenous IRS-1 ubiquitination was detected by immunoblotting with anti-ubiquitin antibody.

Insulin signaling in the skeletal muscle

To investigate the insulin signaling in the skeletal muscle, insulin (10 U/kg) was administered into the retro-orbital sinus of 14-week-old male mice. After 10 min, skeletal muscles (soleus muscle and gastrocnemius and plantaris muscles) were dissected. The isolated muscles were immediately frozen in liquid nitrogen and then stored at −80 °C. Proteins were extracted by homogenizationin lysis buffer (100 mM Tris-Cl, pH 8.3, 25 mM EDTA, protease inhibitor cocktail and phosphatase inhibitors) and subjected to SDS-PAGE.

Measurement of body composition and energy balance

Fat and fat-free masses of 19-week-old male mice that were fed with the HFD for 4 weeks were with a ^1H minispec system (LF90II; Bruker Optik, Ettlingen, Germany). Activity, food consumption, and energy expenditure were assessed in metabolic monitoring system (CLAMS: Columbus Instruments, Columbus, OH, USA) for 4 days (2 days of acclimation followed by 2 days of measurements) at the end of 4 week on the HFD. Energy expenditure and respiratory quotient (RQ) were calculated from the gas exchange data. RQ is the ratio of VCO_2 to VO_2, which changes depending on the energy source that the animal is using. Energy expenditure = (3.815 + 1.232 * RQ) * VO_2. Activity was measured along the x- and z-axes using infrared beams to count the number of beam breaks during the specified measurement period.

Glucose tolerance and insulin tolerance tests

For glucose tolerance tests, 14-week-old male mice that had been fasted overnight received an intraperitoneal injection of D-glucose (2 g/kg body weight). For the insulin tolerance test, insulin (0.75 U/kg for mice fed a regular diet, 1.5 U/kg for mice fad a high fat/high sucrose

NIH-PA Author Manuscript

NIH-PA Author Manuscript

NIH-PA Author Manuscript

diet) were intraperitoneally injected into 14-week-old male mice that had been fed. Blood was obtained from the tail and glucose levels were determined with an automatic glucose monitor.

Measurement of serum samples

Blood samples were collected from the tails of 14-week-old male mice that were fasted overnight. After centrifugation at 1,000 × *g* for 10 min, the supernatants of the blood samples were separated. The serum levels of triacylglycerol, free fatty acids, and total cholesterol were measured with colorimetric assay kits (BioVision, Mountain View, CA). The serum levels of insulin and leptin were determined with the Bio-Plex Pro™ mouse diabetes assay kits (Bio-Rad, Hercules, CA).

Statistical analysis

Statistical values are presented as the mean ± SEM. A two-tailed Student's *t*-test was used to calculate the *P* values.

Supplementary Material

Refer to Web version on PubMed Central for supplementary material.

Acknowledgments

This work was supported by grants awarded to Y.-G. Ko from the National Research Foundation (2011-0030158 and 2011-0017562) and to J. Ma from the National Institutes of Health (HL069000 and AR061385).

References

1. Braun T, Gautel M. Transcriptional mechanisms regulating skeletal muscle differentiation, growth and homeostasis. Nat Rev Mol Cell Biol. 2011; 12:349–361. [PubMed: 21602905]
2. Sandri M. Signaling in muscle atrophy and hypertrophy. Physiology (Bethesda). 2008; 23:160–170. [PubMed: 18556469]
3. Baker J, Liu JP, Robertson EJ, Efstratiadis A. Role of insulin-like growth factors in embryonic and postnatal growth. Cell. 1993; 75:73–82. [PubMed: 8402902]
4. Liu JP, Baker J, Perkins AS, Robertson EJ, Efstratiadis A. Mice carrying null mutations of the genes encoding insulin-like growth factor I (Igf-1) and type 1 IGF receptor (Igf1r). Cell. 1993; 75:59–72. [PubMed: 8402901]
5. Powell-Braxton L, et al. IGF-I is required for normal embryonic growth in mice. Genes Dev. 1993; 7:2609–2617. [PubMed: 8276243]
6. Alzghoul MB, Gerrard D, Watkins BA, Hannon K. Ectopic expression of IGF-I and Shh by skeletal muscle inhibits disuse-mediated skeletal muscle atrophy and bone osteopenia in vivo. Faseb J. 2004; 18:221–223. [PubMed: 14597562]
7. Musaro A, et al. Localized Igf-1 transgene expression sustains hypertrophy and regeneration in senescent skeletal muscle. Nat Genet. 2001; 27:195–200. [PubMed: 11175789]
8. Chambon C, et al. Myocytic androgen receptor controls the strength but not the mass of limb muscles. Proc Natl Acad Sci U S A. 2010; 107:14327–14332. [PubMed: 20660752]
9. Sainz N, et al. Leptin administration favors muscle mass accretion by decreasing FoxO3a and increasing PGC-1alpha in ob/ob mice. PLoS One. 2009; 4:e6808. [PubMed: 19730740]
10. Gardner S, Alzhanov D, Knollman P, Kuninger D, Rotwein P. TGF-beta inhibits muscle differentiation by blocking autocrine signaling pathways initiated by IGF-II. Mol Endocrinol. 2011; 25:128–137. [PubMed: 21106882]
11. Shimizu N, et al. Crosstalk between glucocorticoid receptor and nutritional sensor mTOR in skeletal muscle. Cell Metab. 2011; 13:170–182. [PubMed: 21284984]

NIH-PA Author Manuscript NIH-PA Author Manuscript NIH-PA Author Manuscript

12. Glass DJ. Signalling pathways that mediate skeletal muscle hypertrophy and atrophy. Nat Cell Biol. 2003; 5:87–90. [PubMed: 12563267]
13. Glass DJ. PI3 kinase regulation of skeletal muscle hypertrophy and atrophy. Curr Top Microbiol Immunol. 2010; 346:267–278. [PubMed: 20593312]
14. Clemmons DR. Role of IGF-I in skeletal muscle mass maintenance. Trends Endocrinol Metab. 2009; 20:349–356. [PubMed: 19729319]
15. Otto A, Patel K. Signalling and the control of skeletal muscle size. Exp Cell Res. 2010; 316:3059–3066. [PubMed: 20406633]
16. Ohanna M, et al. Atrophy of S6K1(−/−) skeletal muscle cells reveals distinct mTOR effectors for cell cycle and size control. Nat Cell Biol. 2005; 7:286–294. [PubMed: 15723049]
17. Bodine SC, et al. Akt/mTOR pathway is a crucial regulator of skeletal muscle hypertrophy and can prevent muscle atrophy in vivo. Nat Cell Biol. 2001; 3:1014–1019. [PubMed: 11715023]
18. Hribal ML, Nakae J, Kitamura T, Shutter JR, Accili D. Regulation of insulin-like growth factor-dependent myoblast differentiation by Foxo forkhead transcription factors. J Cell Biol. 2003; 162:535–541. [PubMed: 12925703]
19. Stitt TN, et al. The IGF-1/PI3K/Akt pathway prevents expression of muscle atrophy-induced ubiquitin ligases by inhibiting FOXO transcription factors. Mol Cell. 2004; 14:395–403. [PubMed: 15125842]
20. Sandri M, et al. Foxo transcription factors induce the atrophy-related ubiquitin ligase atrogin-1 and cause skeletal muscle atrophy. Cell. 2004; 117:399–412. [PubMed: 15109499]
21. Bodine SC, et al. Identification of ubiquitin ligases required for skeletal muscle atrophy. Science. 2001; 294:1704–1708. [PubMed: 11679633]
22. Sacheck JM, Ohtsuka A, McLary SC, Goldberg AL. IGF-I stimulates muscle growth by suppressing protein breakdown and expression of atrophy-related ubiquitin ligases, atrogin-1 and MuRF1. Am J Physiol Endocrinol Metab. 2004; 287:E591–601. [PubMed: 15100091]
23. Potthoff MJ, Olson EN, Bassel-Duby R. Skeletal muscle remodeling. Curr Opin Rheumatol. 2007; 19:542–549. [PubMed: 17917533]
24. Murton AJ, Constantin D, Greenhaff PL. The involvement of the ubiquitin proteasome system in human skeletal muscle remodelling and atrophy. Biochim Biophys Acta. 2008; 1782:730–743. [PubMed: 18992328]
25. Kawabe H, Brose N. The role of ubiquitylation in nerve cell development. Nat Rev Neurosci. 2011; 12:251–268. [PubMed: 21505515]
26. Ozato K, Shin DM, Chang TH, Morse HC 3rd. TRIM family proteins and their emerging roles in innate immunity. Nat Rev Immunol. 2008; 8:849–860. [PubMed: 18836477]
27. Kim BW, et al. Lipid raft proteome reveals that oxidative phosphorylation system is associated with the plasma membrane. Expert Rev Proteomics. 2010; 7:849–866. [PubMed: 21142887]
28. Lee CS, et al. TRIM72 negatively regulates myogenesis via targeting insulin receptor substrate-1. Cell Death Differ. 2010; 17:1254–1265. [PubMed: 20139895]
29. Jung SY, Ko YG. TRIM72, a novel negative feedback regulator of myogenesis, is transcriptionally activated by the synergism of MyoD (or myogenin) and MEF2. Biochem Biophys Res Commun. 2010; 396:238–245. [PubMed: 20399744]
30. Cai C, et al. MG53 regulates membrane budding and exocytosis in muscle cells. J Biol Chem. 2009; 284:3314–3322. [PubMed: 19029292]
31. Cai C, et al. MG53 nucleates assembly of cell membrane repair machinery. Nat Cell Biol. 2009; 11:56–64. [PubMed: 19043407]
32. Zhu H, et al. Polymerase transcriptase release factor (PTRF) anchors MG53 protein to cell injury site for initiation of membrane repair. J Biol Chem. 2011; 286:12820–12824. [PubMed: 21343302]
33. Park EY, et al. Crystal structure of PRY-SPRY domain of human TRIM72. Proteins. 2010; 78:790–795. [PubMed: 19967786]
34. Rommel C, et al. Differentiation stage-specific inhibition of the Raf-MEK-ERK pathway by Akt. Science. 1999; 286:1738–1741. [PubMed: 10576741]

NIH-PA Author Manuscript NIH-PA Author Manuscript NIH-PA Author Manuscript

35. Murgia M, et al. Ras is involved in nerve-activity-dependent regulation of muscle genes. Nat Cell Biol. 2000; 2:142–147. [PubMed: 10707084]
36. Ye Y, Rape M. Building ubiquitin chains: E2 enzymes at work. Nat Rev Mol Cell Biol. 2009; 10:755–764. [PubMed: 19851334]
37. Saltiel AR, Kahn CR. Insulin signalling and the regulation of glucose and lipid metabolism. Nature. 2001; 414:799–806. [PubMed: 11742412]
38. Niu W, et al. Maturation of the regulation of GLUT4 activity by p38 MAPK during L6 cell myogenesis. J Biol Chem. 2003; 278:17953–17962. [PubMed: 12637564]
39. Ueyama A, Yaworsky KL, Wang Q, Ebina Y, Klip A. GLUT-4myc ectopic expression in L6 myoblasts generates a GLUT-4-specific pool conferring insulin sensitivity. Am J Physiol. 1999; 277:E572–578. [PubMed: 10484371]
40. Mitsumoto Y, Klip A. Development regulation of the subcellular distribution and glycosylation of GLUT1 and GLUT4 glucose transporters during myogenesis of L6 muscle cells. J Biol Chem. 1992; 267:4957–4962. [PubMed: 1311324]
41. Hotamisligil GS. Inflammation and metabolic disorders. Nature. 2006; 444:860–867. [PubMed: 17167474]
42. Shoelson SE, Lee J, Goldfine AB. Inflammation and insulin resistance. J Clin Invest. 2006; 116:1793–1801. [PubMed: 16823477]
43. Lumeng CN, Saltiel AR. Inflammatory links between obesity and metabolic disease. J Clin Invest. 2011; 121:2111–2117. [PubMed: 21633179]
44. Ouchi N, Parker JL, Lugus JJ, Walsh K. Adipokines in inflammation and metabolic disease. Nat Rev Immunol. 2011; 11:85–97. [PubMed: 21252989]
45. Serra C, et al. Functional interdependence at the chromatin level between the MKK6/p38 and IGF1/PI3K/AKT pathways during muscle differentiation. Mol Cell. 2007; 28:200–213. [PubMed: 17964260]
46. Pete G, et al. Postnatal growth responses to insulin-like growth factor I in insulin receptor substrate-1-deficient mice. Endocrinology. 1999; 140:5478–5487. [PubMed: 10579310]
47. Tamemoto H, et al. Insulin resistance and growth retardation in mice lacking insulin receptor substrate-1. Nature. 1994; 372:182–186. [PubMed: 7969452]
48. Araki E, et al. Alternative pathway of insulin signalling in mice with targeted disruption of the IRS-1 gene. Nature. 1994; 372:186–190. [PubMed: 7526222]
49. Kawaguchi T, et al. Hepatitis C virus down-regulates insulin receptor substrates 1 and 2 through up-regulation of suppressor of cytokine signaling 3. Am J Pathol. 2004; 165:1499–1508. [PubMed: 15509521]
50. Nakao R, et al. Ubiquitin ligase Cbl-b is a negative regulator for insulin-like growth factor 1 signaling during muscle atrophy caused by unloading. Mol Cell Biol. 2009; 29:4798–4811. [PubMed: 19546233]
51. Xu X, et al. The CUL7 E3 ubiquitin ligase targets insulin receptor substrate 1 for ubiquitin-dependent degradation. Mol Cell. 2008; 30:403–414. [PubMed: 18498745]
52. Shi J, Luo L, Eash J, Ibebunjo C, Glass DJ. The SCF-Fbxo40 complex induces IRS1 ubiquitination in skeletal muscle, limiting IGF1 signaling. Dev Cell. 2011; 21:835–847. [PubMed: 22033112]
53. Song R, et al. Central role of E3 ubiquitin ligase MG53 in insulin resistance and metabolic disorders. Nature. 2013; 494:375–379. [PubMed: 23354051]
54. Shim EH, et al. Targeted disruption of hsp70.1 sensitizes to osmotic stress. EMBO Rep. 2002; 3:857–861. [PubMed: 12189176]
55. Yi JS, et al. Ginsenoside Rh2 induces ligand-independent Fas activation via lipid raft disruption. Biochem Biophys Res Commun. 2009; 385:154–159. [PubMed: 19445898]
56. American Diabetes Association. Diabetes Care. 2010; 33 (Suppl 1):S62–S69. [PubMed: 20042775]
57. Weisleder N, et al. Recombinant MG53 protein modulates therapeutic cell membrane repair in treatment of muscular dystrophy. Sci Transl Med. 2012; 4:139ra85.

NIH-PA Author Manuscript

NIH-PA Author Manuscript

NIH-PA Author Manuscript

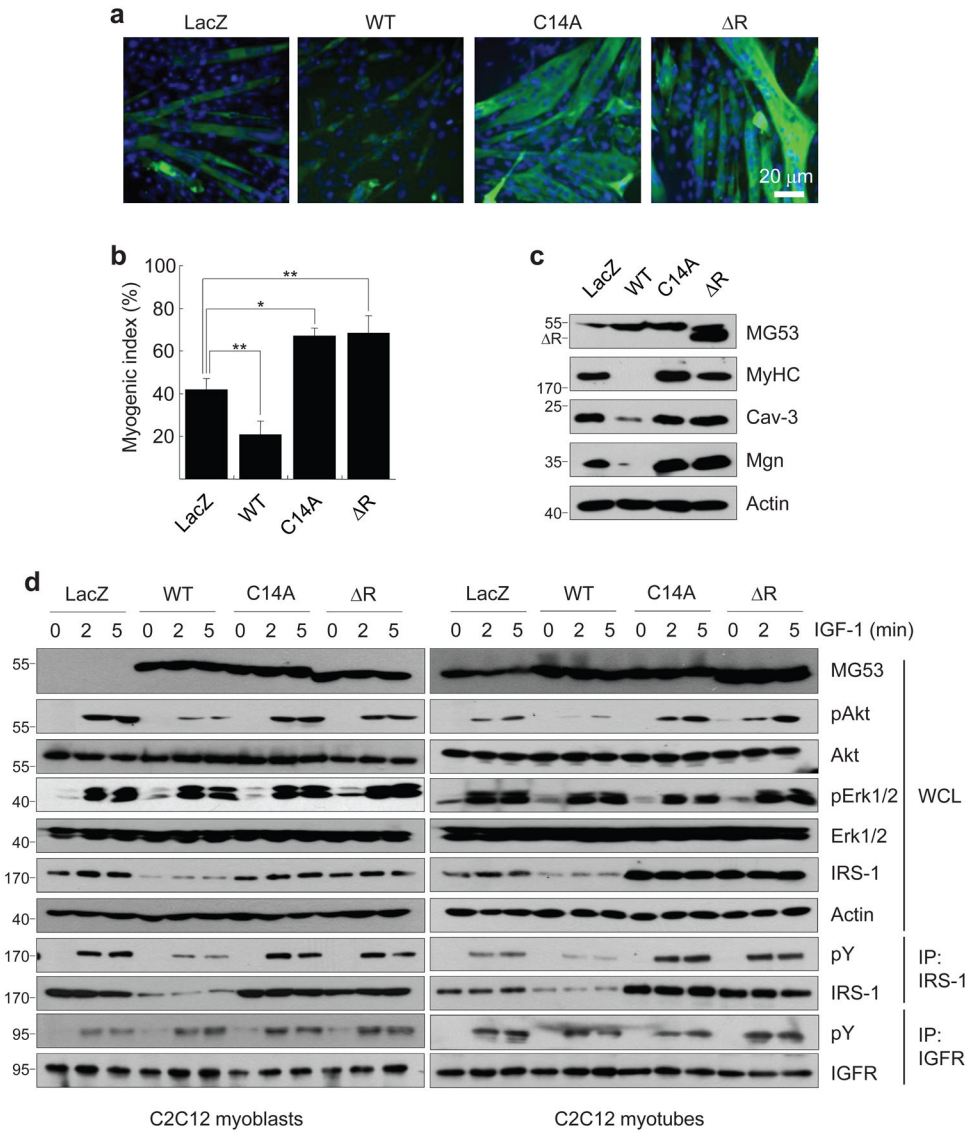

Figure 1. The RING domain of MG53 is required to negatively regulate myogenesis

(ac) C2C12 myoblasts were infected with an adenovirus containing β-galactosidase (LacZ) or the MG53, C14A or ΔR gene and differentiated to myotubes. Myogenesis was assessed by MyHC immunofluorescence and DAPI staining **(a)**; myogenic index **(b);** and immunoblotting for MG53, MyHC, Cav-3 and Mgn, using actin as a loading control **(c)**. Statistical data were obtained from three independent experiments. *t*-test; **P*<0.01 and ***P*<0.05. All data are means ± s.d. **(d)** C2C12 myoblasts were infected with an adenoviral LacZ or MG53, C14A or ΔR and then further incubated (for myoblasts, left panel) or differentiated (for myotubes, right panel). After serum starvation, the myoblasts or myotubes were elicited by IGF-1 treatment for the indicated times. MG53, pAkt, total Akt, pERK1/2, total ERK1/2 and IRS-1 were analyzed by immunoblotting, using actin as a loading control. Tyrosine phosphorylation (pY) of IGFR and IRS-1 was determined by immunoprecipitation. IP, immunoprecipitation; WCL, whole cell lysates.

NIH-PA Author Manuscript

NIH-PA Author Manuscript

NIH-PA Author Manuscript

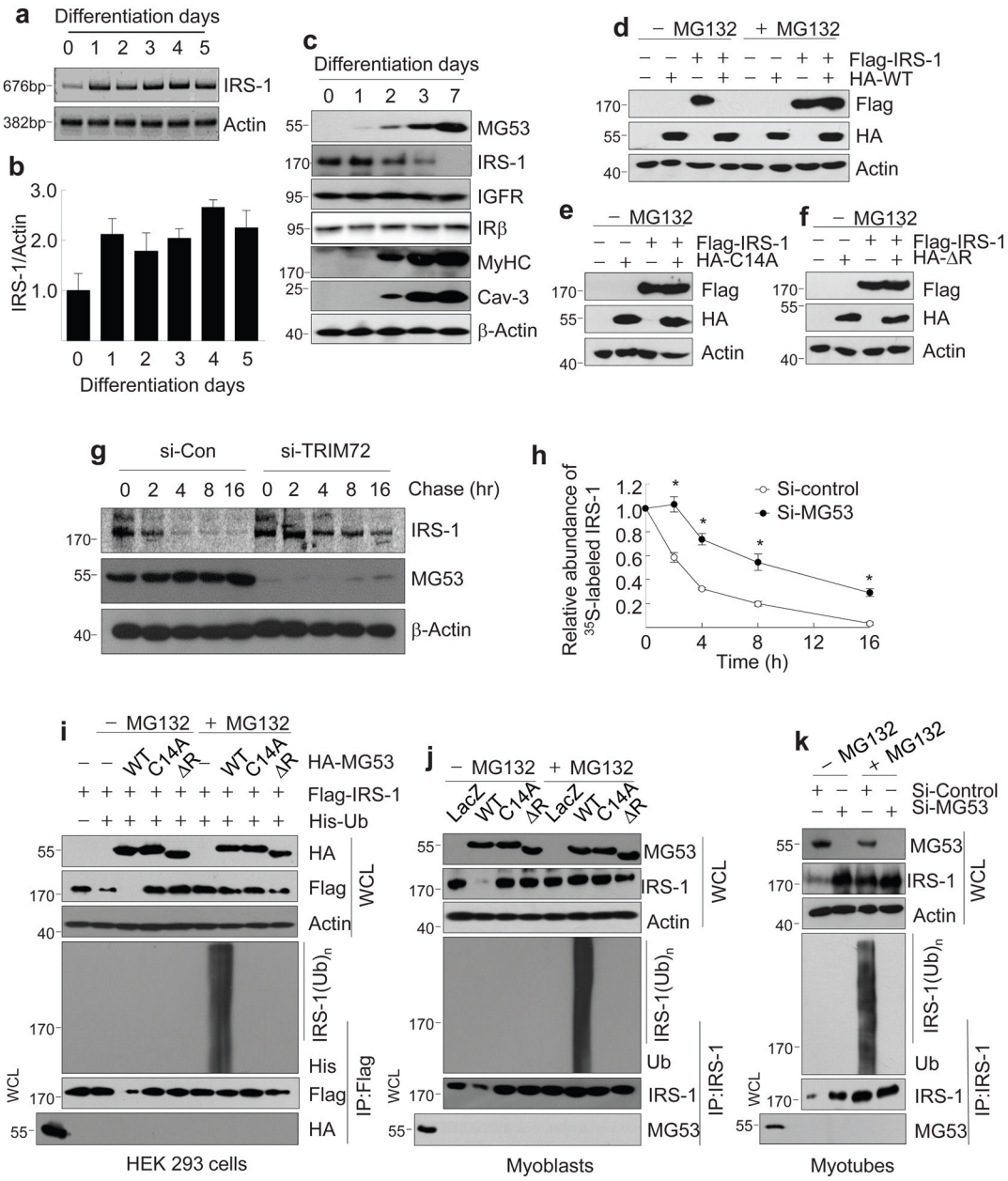

Figure 2. MG53 is an E3 ligase enzyme inducing IRS-1 ubiquitination

(a) Reverse transcription-polymerase chain reaction (RT-PCR) analysis of IRS-1 during C2C12 myogenesis, using actin as a loading control. C2C12 myoblasts were differentiated to myotubes for the indicated times. (b) Quantitative real-time PCR of IRS-1 during C2C12 myogenesis for the indicated times. IRS-1 mRNA was normalized to actin mRNA. Statistical data were obtained from three independent experiments. All data are means ± s.d. **(c)** Immunoblotting analysis of MG53, Mgn, MyHC, Cav-3, IRβ, IGFR and IRS-1 during C2C12 myogenesis, using actin as a loading control. **(d-f)** IRS-1 is degraded by MG53 but not by C14A or ΔR. Flag-IRS-1 was co-transfected with HA-MG53 **(d)**, C14A **(e)** or ΔR **(f)** into HEK 293 cells. With or without MG132 treatment, the expression levels of IRS-1 and MG53 were determined by immunoblotting. (**g, h**) The degradation rate of IRS-1 protein was determined in si-control or si-MG53-treated C2C12 myotubes by pulse-chase analysis

NIH-PA Author Manuscript

NIH-PA Author Manuscript

NIH-PA Author Manuscript

with [^{35}S]methionine and [^{35}S]cysteine. The IRS-1 protein was immunoprecipitated at the indicated times, separated by SDS-PAGE and detected by autoradiography (g). The relative abundance of labeled IRS-1 protein was calculated from three independent experiments (h).t-test; $p<0.05$ (control versus si-MG53). All data are means ± s.d. **(i)** MG53 induces IRS-1 ubiquitination in HEK 293 cells. Flag-IRS-1, His-Ubiquitin and HA-MG53, C14A or ΔR were co-transfected into HEK 293 cells in the indicated combinations. After MG132 treatment, IRS-1 ubiquitination was determined by immunoprecipitation with an anti-Flag antibody. **(j)** C2C12 myoblasts were infected with adenoviral LacZ or MG53, C14A or ΔR. After MG132 treatment, IRS-1 ubiquitination was determined by immunoprecipitation. **(k)** C2C12 myoblasts were treated with si-MG53 (200 nM) and differentiated to myotubes. After MG132 treatment, IRS-1 ubiquitination was determined by immunoprecipitation.

NIH-PA Author Manuscript

NIH-PA Author Manuscript

NIH-PA Author Manuscript

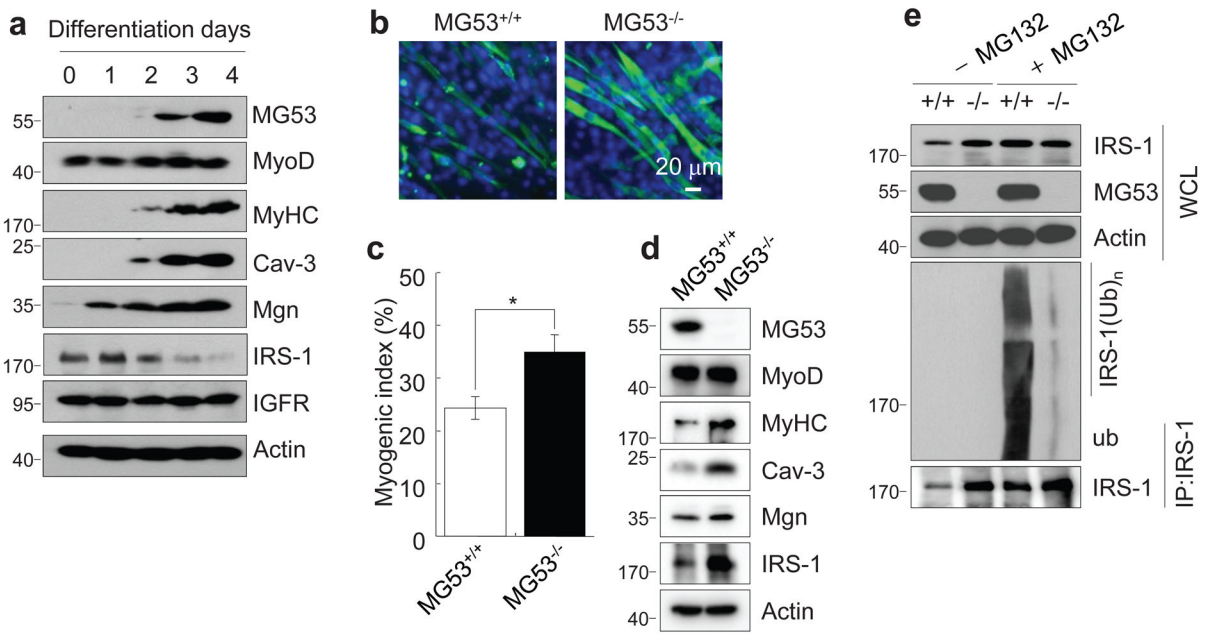

Figure 3. IRS-1 ubiquitination is abrogated in MyoD-driven myotubes of MEFs

(a) The MG53 protein level is increased during MyoD-driven myogenesis of MEFs. MEFs were isolated from wild-type mice embryos, infected with adenovirus with MyoD, and differentiated to myotubes for the indicated times. The expression levels of MG53, MyoD, MyHC, Cav-3, Mgn, IRS-1 and IGFR were monitored by immunoblotting, using actin as a loading control. **(b-d)** MG53 knockout enhances the MyoD-driven myogenesis of MEFs. $MG53^{+/+}$ and $MG53^{-/-}$ MEFs were infected with adenoviral MyoD and differentiated to myotubes for 4 days. Myogenesis was assessed by MyHC immunofluorescence and DAPI staining **(b)**; the myogenic index **(c);** and immunoblotting for MG53, MyoD, MyHC, Cav-3, Mgn, IRS-1 and actin **(d)**. The myogenic index in the MyHC-stained cells was calculated at least from the six different fields. *t*-test; $*P<0.01$. All data are means ± s.d. **(e)** MG53 knockout abolishes IRS-1 ubiquitination in MyoD-driven myotubes of MEFs. Myotubes of MyoD-overexpressing $MG53^{+/+}$ and $MG53^{-/-}$ MEFs were treated with or without MG132. IRS-1 ubiquitination was determined by immunoprecipitation.

NIH-PA Author Manuscript

NIH-PA Author Manuscript

NIH-PA Author Manuscript

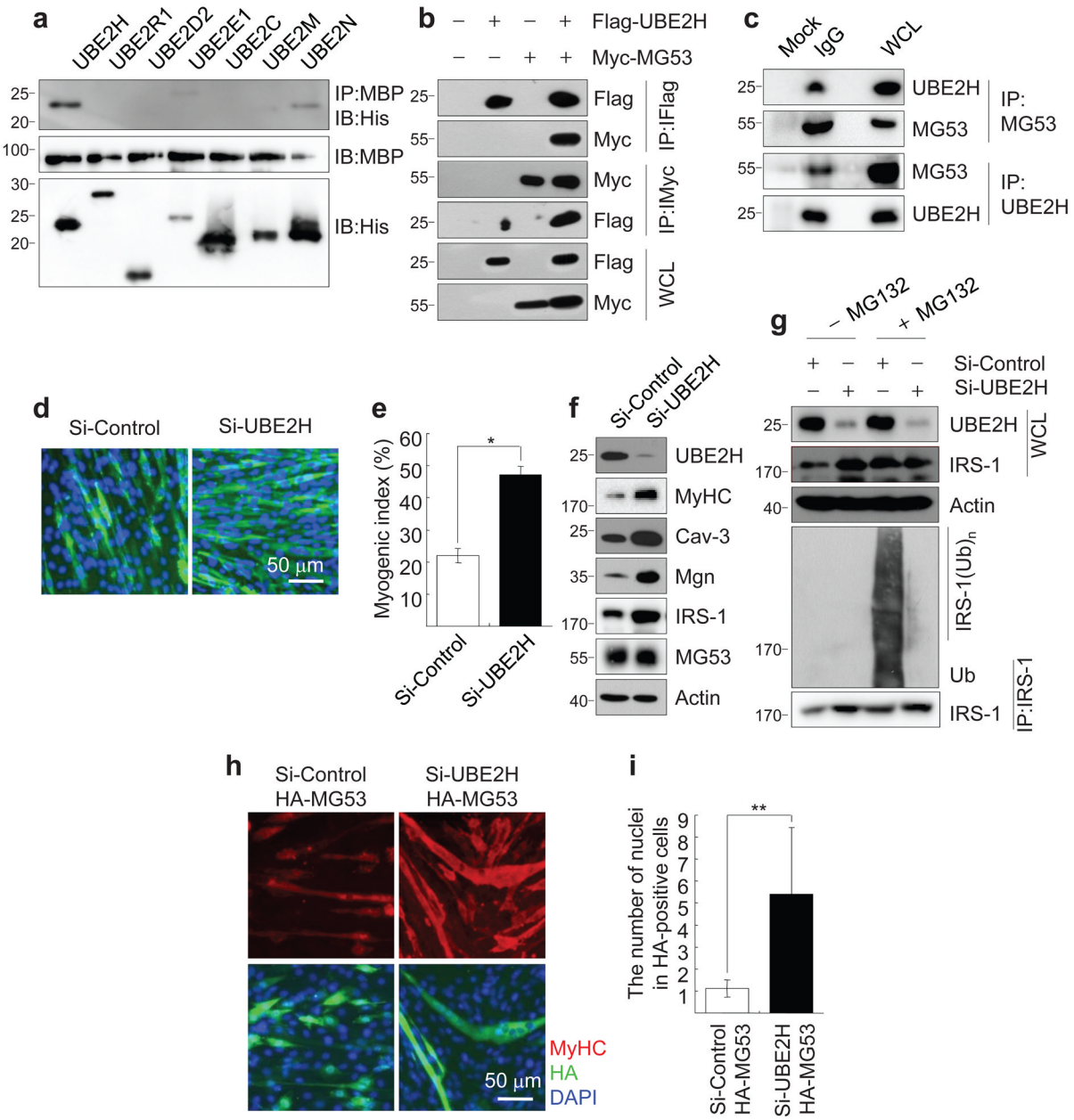

Figure 4. UBE2H is an E2 enzyme for MG53-mediated IRS-1 ubiquitination

(a) *In vitro* binding assay of MG53 with various E2 enzymes. The mixtures of MBP-MG53 and various His-E2 enzymes were immobilized on an amylose resin, and the interaction was analyzed by immunoblotting. **(b)** Myc-MG53 and Flag-UBE2H were co-transfected into HEK 293 cells in different combinations. The molecular interaction between MG53 and UBE2H was monitored by reciprocal immunoprecipitation. **(c)** The molecular association of MG53 with UBE2H by reciprocal endogenous immunoprecipitation from differentiated C2C12 myotubes. **(d-f)** C2C12 myoblasts were treated with si-control or si-UBE2H (200 nM) and then differentiated to myotubes. Myogenesis was assessed by MyHC immunofluorescence and DAPI staining **(d)**, the myogenic index **(e)** and immunoblotting **(f)**. The myogenic index in the MyHC-stained cells was calculated at least from the six different fields. *t*-test; $*P<0.01$. All data are means ± s.d. **(g)** After UBE2H knockdown, C2C12

NIH-PA Author Manuscript

NIH-PA Author Manuscript

NIH-PA Author Manuscript

myotubes were treated with MG132, and IRS-1 ubiquitination was determined by endogenous immunoprecipitation. **(h,i)** HA-MG53 was transiently co-transfected along with si-control or si-UBE2H (200 nM) in C2C12 myoblasts. The myoblasts were further differentiated to myotubes and analyzed by MyHC and HA immunofluorescence **(h)**. The nuclei were stained with DAPI. The number of nuclei in HA-positive cells was calculated in three independent microscopic fields **(i)**. *t*-test; $*P<0.01$. All data are means ±s.d.

NIH-PA Author Manuscript

NIH-PA Author Manuscript

NIH-PA Author Manuscript

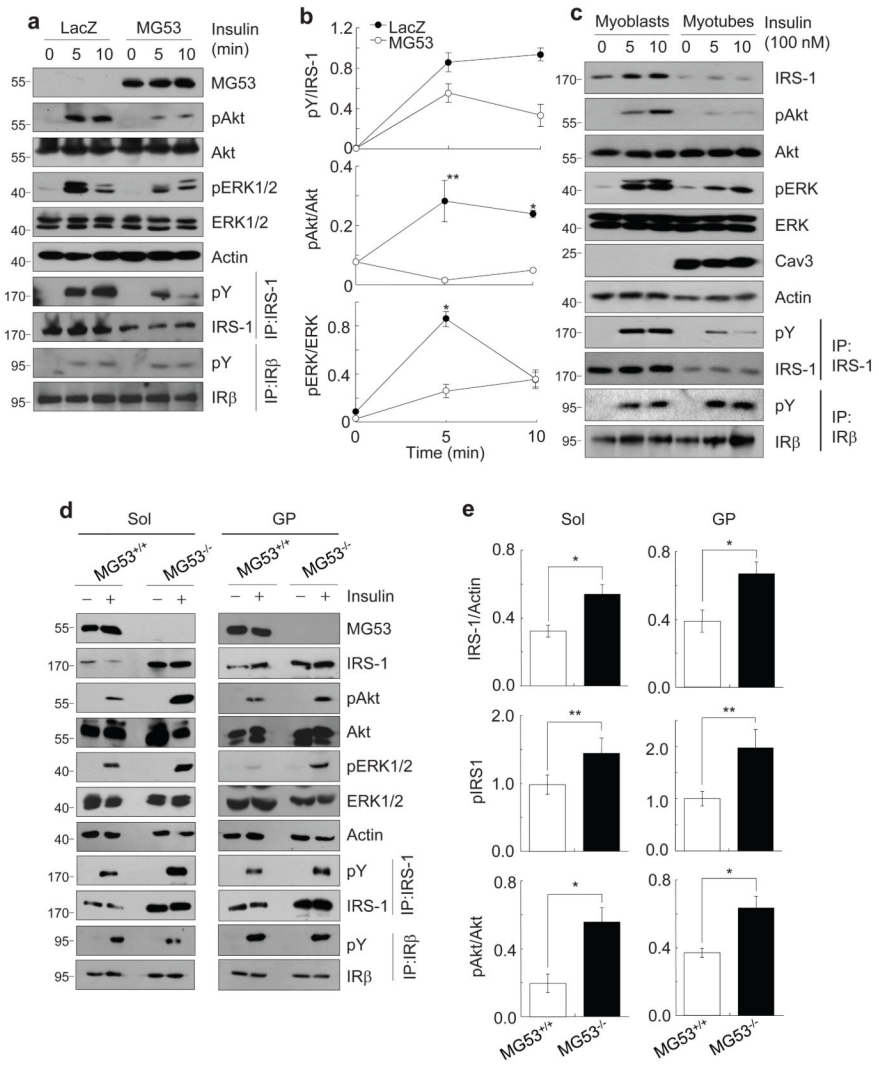

Figure 5. Insulin signaling is increased in the skeletal muscle of MG53 knockout mice

(**a,b**) MG53 was adenovirally overexpressed in C2C12 myoblasts. The myoblasts were then serum-starved and elicited by insulin (100 nM) for the indicated times. MG53, pAkt, total Akt, pERK1/2, total ERK1/2 and actin was monitored by immunoblotting. The tyrosine phosphorylation of IRS-1 was determined by immunoprecipitation (a). The pIRS-1, pAkt and pERK1/2 level were statistically determined (n=3 for each condition) (b). *t*-test; $^{*}p<0.05$ and $^{**}p<0.01$ (LacZ versus MG53). All data are means ± s.d. **(c)** C2C12 myoblasts were differentiated to myotubes for 4 days. The myoblasts and myotubes were serum-starved and elicited by insulin for indicated times. IRS-1, pAkt, total Akt, pERK1/2, total ERK1/2, Cav-3 and actin were monitored by immunoblotting. The tyrosine phosphorylation of IRS-1 was determined by immunoprecipitation. **(d,e)** After intravenous injection of insulin, both the soleus (Sol) and gastrocnemius-plantaris (GP) were isolated from 8-week-old male $MG53^{+/+}$ and $MG53^{-/-}$ mice. Insulin signaling was analyzed by immunoblotting and immunoprecipitation (**d**). The IRS-1, pIRS-1 and pAkt levels were statistically assessed (*n*=5 for each group). *t*-test; $^{*}p<0.05$ and $^{**}p<0.01$. All data are means ±s.d. (**e**).

NIH-PA Author Manuscript

NIH-PA Author Manuscript

NIH-PA Author Manuscript

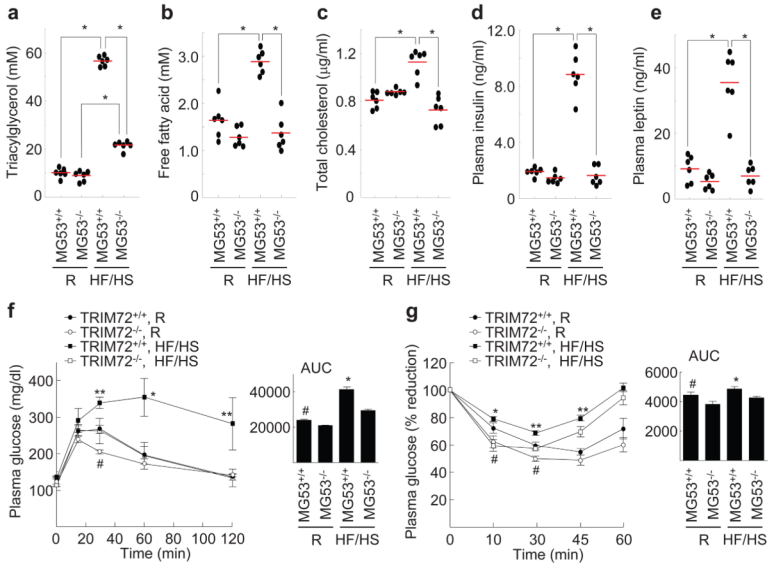

Figure 6. Insulin resistance does not develop in MG53$^{-/-}$ mice

Four-week-old male MG53$^{+/+}$ and MG53$^{-/-}$ mice (*n*=6 for each group) were fed a regular diet or a HF/HS diet for 10 weeks. **(a-e)** Serum was obtained from overnight-fasted mice. The concentration of triacylglycerol **(a)**, free fatty acid **(b)**, total cholesterol **(c)**, insulin **(d)** and leptin **(e)** were measured. R, regular diet; HF/HS, high fat/high sucrose diet. *t*-test; $^{*}P<0.01$. **(f, g)** Glucose tolerance **(f)** and insulin tolerance **(g)** tests were then performed in the regular diet (R)- and the HF/HS (HF/HS)-fed MG53$^{+/+}$ and MG53$^{-/-}$ mice (*n*=6 for each group). AUC indicates the area under the curve. *t*-test; $^{*}p<0.05$ and $^{**}p<0.01$ (MG53$^{-/-}$ HF/HS versus MG53$^{+/+}$ HF/HS) and, $^{\#}$p<0.05 (MG53$^{-/-}$ R versus MG53 $^{+/+}$R). All data are means ±s.d.

NIH-PA Author Manuscript

NIH-PA Author Manuscript

NIH-PA Author Manuscript

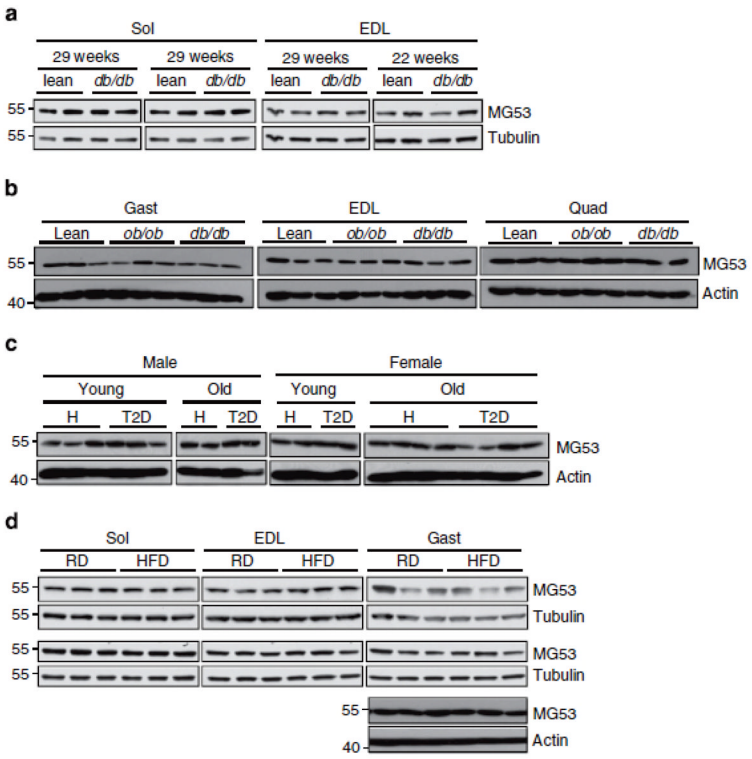

Figure 7. MG53 protein in animals and humans with metabolic disorders

(***a***) Immunoblots of soleus (Sol) and EDL derived from littermates of *db/db* and lean control mice at ages of 22 and 29 weeks. (***b***) Study with *ob/ob*, *db/db* and lean mice purchased from Jackson Lab also did not reveal significant changes in MG53 expression in EDL, gastrocnemius (Gast) and quadriceps (Quad) at 8-week age. (***c***) Skeletal muscle (*vastus lateralis*) biopsies were obtained from human patients with type 2 diabetes (T2D) and healthy (H) controls. Protein expression levels were analyzed by immunoblotting using actin as a loading control. T2D was diagnosed using American Diabetes Association criteria [56]. 'Young' refers to ages between 28 and 55 years, 'Old' indicates ages between 65 and 82. **(*d*)** Sol, EDL and Gast obtained from littermates of wild type mice (C57B/6J) following 1-week treatment of regular chow diet (RD) or high fat diet (HFD) starting from 25 days after birth (*top panel*) or 8 weeks after birth (*middle panel*). Separate trials were performed with 8-week old mice following 4-weeks treatment with HFD (*bottom panel*). MG53 protein levels in the different types of skeletal muscle shown in Figure 7a–d were statistically not different between control and animal models with metabolic disorders or human diabetes patients.

NIH-PA Author Manuscript

NIH-PA Author Manuscript

NIH-PA Author Manuscript

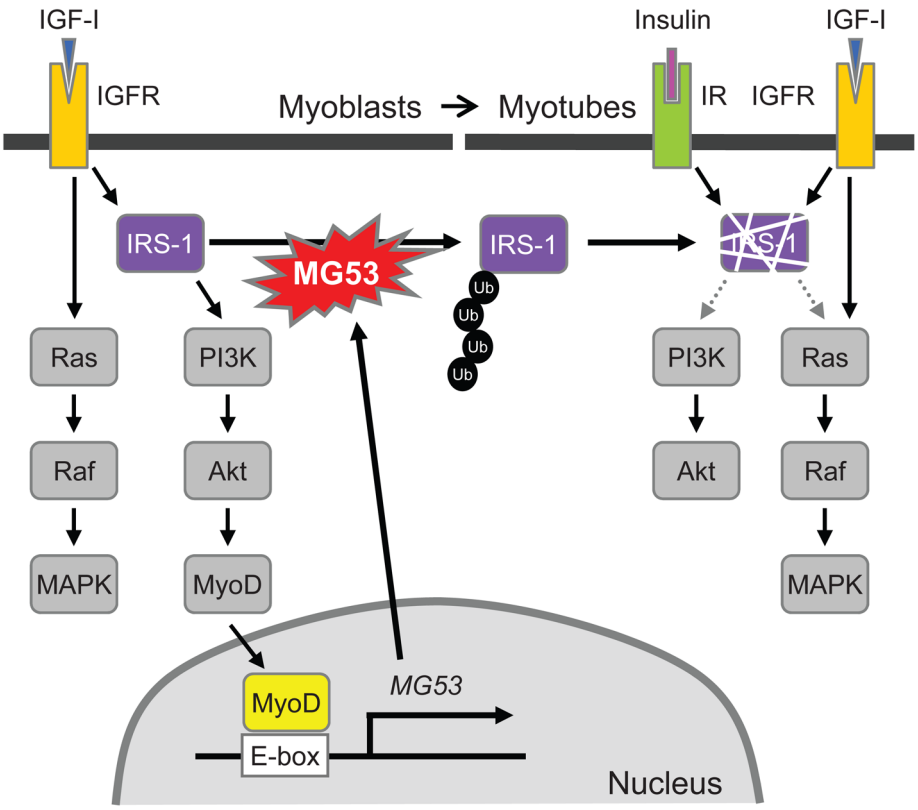

Figure 8.

MG53-mediated negative feedback regulation of skeletal myogenesis. MG53 transcription is initiated by an IGFR-IRS-1-Akt-MyoD pathway during skeletal myogenesis. The MG53 protein interacts with, ubiquitinates and degrades IRS-1, leading to the blockage of IGF and insulin signaling in fully-differentiated myotubes.